

***Ab initio* study of phase transformations in boron nitride**

W. J. Yu and W. M. Lau*

Department of Physics and Materials Science and Technology Research Centre, The Chinese University of Hong Kong, Hong Kong, China

S. P. Chan and Z. F. Liu

Department of Chemistry, The Chinese University of Hong Kong, Hong Kong, China

Q. Q. Zheng

Institute of Solid State Physics, Chinese Academy of Sciences, 230031 Hefei, China

(Received 31 July 2002; published 27 January 2003)

The structural properties and phase stability of the four common polytypes of boron nitride, cubic zinc blende (*c*-BN), hexagonal (*h*-BN), wurtzite (*w*-BN) and rhombohedral (*r*-BN), are studied by *ab initio* calculations. Electronic energies are calculated using an ultra soft pseudopotential method under the density-functional theory, and phonon dispersions are calculated using the first-principles force-constant method. The *p*-*T* phase diagrams of these four boron nitride phases are constructed with the quasiharmonic approximation. Direct compression simulations are then performed to find probable phase transformation paths among these polytypes, with additional energy calculations of plausible transition structures. The *c*-BN phase is the most thermodynamically stable in ambient conditions among these four polytypes, and the transformation between *r*-BN and *c*-BN has the smallest energy barrier. Direct transformation between *h*-BN and *c*-BN is far less favorable than indirect transformation, with *w*-BN or *r*-BN as an intermediate. The presence of structural defects is a key attribute in reducing the energy barrier of phase transformation. The results in this work offer theoretical clues to experimental data on *c*-BN film growth, particularly the absence of *w*-BN.

DOI: 10.1103/PhysRevB.67.014108

PACS number(s): 64.60.-i, 64.70.Kb, 61.50.Ks, 63.20.Dj

I. INTRODUCTION

The formation of cubic boron nitride (*c*-BN), which is isoelectronic to diamond, has been investigated extensively because *c*-BN has fascinating properties such as hardness only second to diamond, chemical inertness far superior to diamond, high thermal conductivity, large band gap with shallow *n*- and *p*-type dopants, and low dielectric constant.¹ Although boron nitride has no natural abundance, the compound can be synthesized in both powder and thin-film forms.² In boron nitride synthesis, there are four primary crystalline phases that include the hexagonal (*h*-BN), rhombohedral (*r*-BN), cubic zinc-blende (*c*-BN), and wurtzite (*w*-BN) forms. The first two forms are constructed by flat sheets of BN having *sp*² bonds, with a large separation between two adjacent sheets. They thus have relatively low densities, and are referred to as light phases in this work. The latter two forms are constructed by *sp*³ bonds and are denser and harder than the other two forms. Hence, these two phases are referred to as dense phases in this work. The lattice structures are shown in Fig. 1. Recent experimental and theoretical studies have consistently shown that *c*-BN is the thermodynamically stable phase in ambient conditions.^{3–6} However, in practical boron nitride synthesis, which takes place near atmospheric pressure in a wide temperature range, *sp*² BN is commonly formed. In addition, it has also been shown experimentally that *c*-BN can be transformed into *h*-BN by moderate heating⁷ and *r*-BN by laser heating,⁸ both at atmospheric pressure. A coherent model for explaining the phase transformations among the polytypes of BN is required.

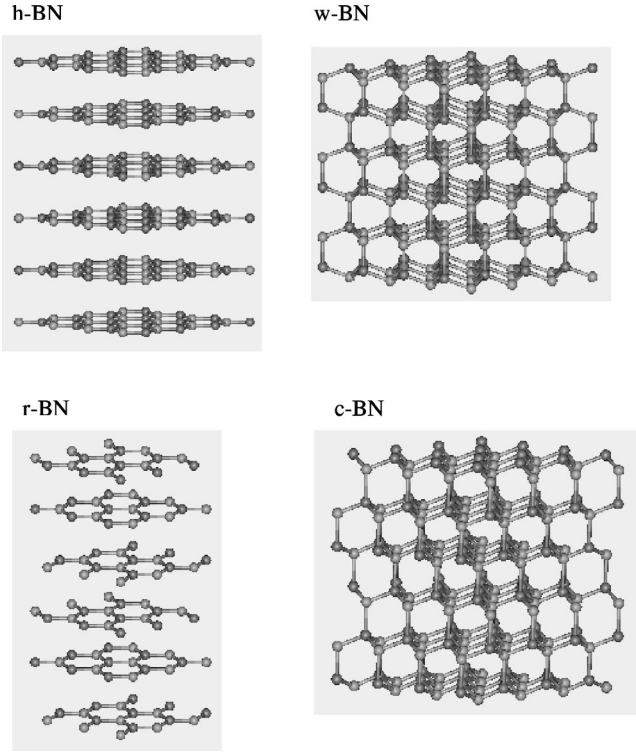
Since experimental synthesis of pure *c*-BN, *w*-BN, and

r-BN phases have encountered practical difficulties in various aspects, several research groups have resorted to the computational analysis of some of these phases. For example, Kern *et al.*⁵ conducted a comprehensive study of the lattice dynamics and stability of *c*-BN and *h*-BN by *ab initio* calculations with an ultrasoft pseudopotential,⁹ and constructed a phase diagram of these two polytypes. More recently, Ohba *et al.*⁶ extended the analysis by including *w*-BN into the phase comparison. However, a complete picture of transformation pathways among *c*-BN, *w*-BN, *r*-BN, and *h*-BN has not yet been drawn. From the lattice structures shown in Fig. 1, it is reasonable to infer that the transformation of *c*-BN to *r*-BN and *w*-BN to *h*-BN occur through flattening the BN (111) planes of the dense phases. Intuitively, these two phase transformation processes should have relatively small energy barriers, relative to a direct transformation between *c*-BN to *h*-BN. A clarification of these phase transformation pathways is the main objective of this present work.

In this work, we use the same first-principles method employed by Kern *et al.*⁵ to calculate the electronic energy of all four polytypes. For phonon-dispersion analysis, we use the approach that has recently been developed and applied to *c*-BN successfully by Parlinski.¹⁰ Compression simulations are then conducted for the elaboration of phase transformation conditions, and additional energy calculations are used to construct pathways among these four most common polytypes of BN.

II. COMPUTATIONAL METHODS

For the construction of the phase transitions among the polytypes of boron nitrides, the Gibbs free energy

FIG. 1. Crystal structures of *h*-BN, *w*-BN, *r*-BN, and *c*-BN.

$$G = F + PV \quad (1)$$

must be calculated for each phase at different pressures and temperatures. In this equation, F is the Helmholtz free energy which is equal to

$$F(T, V) = E_o(V) + F_{vib}(T, V) + U_o(V) + F_A(V). \quad (2)$$

The first term E_o is the total electronic energy and the third term U_o is the zero-point energy. The sum of the second and third terms represents the harmonic vibration energy, and the last term F_A is the anharmonic part of the free energy. In this work, E_o is evaluated by first-principles calculations in the framework of the density-functional theory with the local-density approximation, using the Vienna *ab initio* simulation package (VASP).¹¹ For *c*-BN and *h*-BN, the calculations are the same as those of Kern *et al.*⁵ except that the cutoff energy used in the present work is 450 eV instead of 350 eV.

The two vibration energy terms are approximated by

$$F_{vib}(T, V) = \int_{\Omega} k_B T \ln[1 - \exp(-\hbar \omega / kT)] g(V, \omega) d\omega \quad (3)$$

and

$$U_{zero} = \frac{1}{2} \int_{\Omega} \hbar \omega g(V, \omega) d\omega, \quad (4)$$

where $g(V, \omega)$ is the phonon density of states (DOS) in a fixed volume V . The phonon DOS is calculated with a direct *ab initio* force-constant approach in the following sequence of steps: (i) modeling the solid with a supercell, (ii) displac-

ing one atom of the supercell at a time, (iii) estimating the induced force by the Hellmann-Feynman theorem, (iv) forming the force-constant matrices and dynamical matrices, and (v) solving the dynamical matrices. In practice, the phonon software package written by Parlinski for calculations in this approach, which has already been shown successfully¹⁰ in calculating the phonon DOS of *c*-BN, is used in this work for the calculations of the phonon DOS of all four polytypes of BN. In these calculations, a $2 \times 2 \times 2$ simple cubic supercell containing 64 atoms is used for *c*-BN, a $4 \times 4 \times 1$ supercell containing 64 atoms for *h*-BN, a $4 \times 4 \times 1$ supercell with the space group $P6_3mc/C_{6v}^4$ for *w*-BN, and a $2 \times 2 \times 2$ supercell of 16 atoms with the $R3m/C_{3v}^5$ space group for *r*-BN. The effective charge used in the phonon DOS calculations is the same as that used by Parlinski in his *c*-BN study; the rationale can be found in his work.¹⁰

Finally, the anharmonic term F_A is estimated with a simplified approach of Wallace¹²:

$$F_A = A_2 T^2, \quad (5)$$

where the coefficient A_2 is given by the following empirical relationship:

$$A_2 = \frac{3k_B}{\Theta_H} (0.0078 \langle \gamma \rangle - 0.0154). \quad (6)$$

In this empirical relationship, the average Gruneisen parameter $\langle \gamma \rangle$ is given by

$$\langle \gamma \rangle = - \frac{d \ln \Theta_H}{d \ln V} \quad (7)$$

and the high-temperature harmonic Debye temperature Θ_H by

$$\Theta_H = \frac{\hbar}{k_B} \left(\frac{5}{3} \langle \omega^2 \rangle \right)^{1/2}, \quad (8)$$

where $\langle \omega^2 \rangle$ is the average squared harmonic phonon frequency.

With these energy attributes, pressure p is calculated from the Helmholtz free energies at different volumes for a certain temperature T :

$$p = -(\partial F / \partial V)_T. \quad (9)$$

The pressure where the Gibbs free energies of two phases become the same gives the coexistence point of these two phases at temperature T . The points accumulated by repeating this procedure at different temperatures form a p - T phase diagram.

III. RESULTS AND DISCUSSION

A. Equilibrium properties and phonon dispersion of *c*-BN, *h*-BN, *r*-BN and *w*-BN

In Table I, the equilibrium lattice constants, the total energy, and free energy for *c*-BN, *h*-BN, *w*-BN, and *r*-BN are listed. The results confirm that *c*-BN has the lowest energy

TABLE I. Lattice constants and structural energies of boron nitride.

	<i>c</i> -BN	<i>h</i> -BN	<i>w</i> -BN	<i>r</i> -BN
Supercell size (Å)				
<i>a</i>	7.15	9.92	10.07	4.96
<i>b</i>	7.15	9.92	10.07	4.96
<i>c</i>	7.15	6.49	4.17	19.30
<i>V</i> (Å ³ /atom)	5.71	8.65	5.72	8.57
<i>a</i> (Å)	3.574	2.481	2.518	2.480
	3.615 ^a	2.504 ^a	2.551 ^a	2.504 ^a
<i>c</i> (Å)		6.491	4.167	9.65
		6.656 ^a	4.210 ^a	9.99 ^a
<i>E_o</i> (eV/atom)	-8.020	-7.973	-8.001	-7.976
<i>A</i> (eV/atom)	-7.966	-7.921	-7.948	-7.924

^aExperimental results by Kurdyumov *et al.* (Ref. 22).

among the four polytypes, which is in agreement with both the experimental results and recent theoretical calculations.^{3–6}

The phonon-dispersion spectra and DOS for all four polytypes are shown in Fig. 2. The data for *c*-BN and *h*-BN are virtually the same as those reported by Kern *et al.*,⁵ except that the amplitudes of our phonon-dispersion spectra are smaller than those of the counterparts of Kern *et al.* by about a factor of 3. On the other hand, our data for *c*-BN are the same as those reported by Parlinski,¹⁰ which supports our correct usage of Parlinski's method in estimating the phonon properties of the four polytypes of BN. Since vibration energies are derived by the phonon DOS, scaling the amplitude of the phonon DOS will lead to an incorrect scaling of these two energy terms relative to the electronic energy term. As such, the *p*-*T* phase diagrams will be affected.

By comparing the phonon data of the different polytypes in Fig. 2, one can see that the phonon dispersion spectra of *h*-BN and *r*-BN are similar, with both of them having peaks at frequencies of 10 THz, 18 THz and 40 THz. For both polytypes, all peaks are very sharp and the peak at 40 THz is the highest one. A similarity also exists in the phonon-dispersion spectra of *c*-BN and *w*-BN, with both having an intense peak at 30 THz, as a transverse-optical (TO) phonon peak, and a broad peak at lower frequencies.

In addition to the above data descriptions and analysis, the optical vibration modes of all four BN polytypes at the Γ point are summarized in Table II, which also includes all relevant experimental and theoretical data in the literature.^{5,8,13–17} The *c*-BN and *h*-BN data of the present work are consistent with all experimental and theoretical data for these two phases. Our data on *w*-BN compare well with those from a very recent theoretical study.⁶ As for *r*-BN, our data are the first set of theoretical results in this subject and agree well with the experimental data of Liu *et al.*⁸

The consistency of our data on equilibrium properties and phonon-dispersion properties in reference to those in the literature supports our calculation methodologies, and the subsequent analysis of the phase properties and phase transformation of the four polytypes of BN.

B. Phase diagrams of *c*-BN, *h*-BN, *r*-BN and *w*-BN

Once the Gibbs free energies of each phase as a function of temperature and pressure are calculated, the pressure and temperature attributes for a coexistence point of each pair of phases can be mapped by finding the *p*-*T* condition under which the Gibbs free energies of the two phases are the same. For example, the Gibbs free energies for *c*-BN and *h*-BN at 1660 K as a function of pressure and those for *c*-BN and *r*-BN at 1750 K are shown in Fig. 3. These two sets of data show that at *p*=0, *c*-BN and *h*-BN coexist at 1660 K, whereas the coexistence temperature for *c*-BN and *r*-BN is 1750 K. Since *h*-BN and *r*-BN have very similar cohesive energies and phonon-dispersion properties, their Gibbs free energies are also similar. For example, the cohesive energy of *r*-BN is lower than that of *h*-BN by 0.003 eV/atom, and its Gibbs free energy at *p*=0 is 0.008 eV/atom lower than that of *h*-BN at 1160 K, same as that of *h*-BN at 1250 K, and higher than that of *h*-BN by 0.002 eV/atom at 1660 K and by 0.003 eV/atom at 1750 K. As for *w*-BN, its cohesive energy and Gibbs free energy at *p*=0 are always about 0.018 eV/atom higher than those of *c*-BN in the entire temperature range.

The (*p*, *T*) phase diagram is constructed by accumulating coexistence points for each pair of phases at different temperatures. The results are summarized in Fig. 4. Comparing some of them with the relevant data in the literature can support the appropriateness of these data. For example, our coexistence temperature at *p*=0 for *c*-BN and *h*-BN is 1660 K. In comparison, it is 1440 K in the theoretical study by Kern *et al.*,⁵ 1570 K by Solozhenko and Leonidov,¹⁸ and 1804 K by Kuznetsov *et al.*¹⁹ In view of the differences between our data and those of Kern *et al.*⁵ in the amplitude of the phonon-dispersion spectra, we suspect that our data are more accurate than those of Kern *et al.* There are also experimental data in the literature, but most of them were measured for *c*-BN/*h*-BN transformation in the presence of catalysts or other chemical agents. As for direct transformation, we note that Sachdev *et al.*⁷ demonstrated experimentally the transformation of *c*-BN crystals in three different crystal sizes (about 1, 60, and 600 μ m) to *h*-BN by heating *c*-BN with a standard dynamic thermal analysis procedure. The respective onset transformation temperatures are about 1200, 1600, and 1800 K for the crystals of 1, 60 and 600 μ m in size. It is plausible that the smaller crystals have more defects, including surface defects per unit volume, and are thus more ready for transformation. In a close examination of the experimental results, we also see that for the largest crystals, there is a significant delay from the time when the sample temperature reaches 1800 K to the time when the transformation occurs. This suggests that the transformation is barred by an activation energy, and yet a nucleation process that provides a pathway to reduce the nominal activation energy triggers the transformation.

In addition to citing the above experimental data on *c*-BN/*h*-BN transformation, we like to remark that Liu *et al.*⁸ experimentally transformed *c*-BN crystals by laser heating them at 1795 ± 80 K to a mixture of *c*-BN and *r*-BN. Our coexistence temperature at *p*=0 for *c*-BN/*r*-BN is about 1750 K.

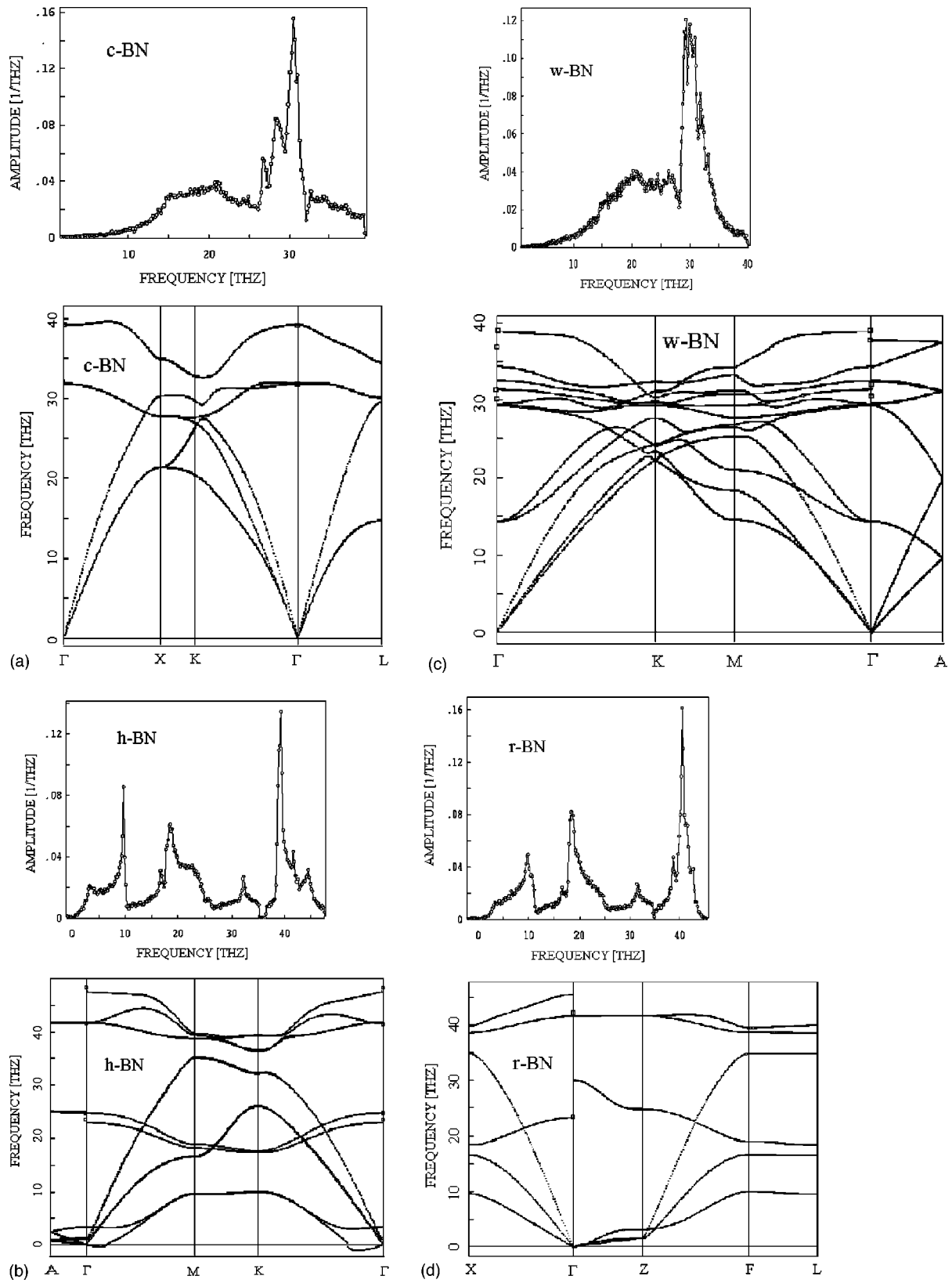
FIG. 2. Phonon density of states and dispersion spectra of *c*-BN, *w*-BN, *h*-BN, and *r*-BN.

TABLE II. Optical vibration modes of BN at Γ point (LO, longitudinal optical modes; TO, transverse optical modes).

	ω_{LO} (cm ⁻¹)		ω_{TO} (cm ⁻¹)	
<i>c</i> -BN	1308		1061	
	1308 ^a		1066 ^a	
	1305 ^b		1055 ^b	
<i>h</i> -BN	A_{2u} : 783	E_{1u} : 1587	A_{2u} : 757	E_{1u} : 1366
	828 ^c	1610 ^c	783 ^c	1367 ^c
<i>w</i> -BN	E_1 : 1288	A_1 : 1250	E_1 : 1085	A_1 : 1047
	1295 ^d	1230 ^d		
	1285 ^e	1285 ^e	1053 ^e	1006 ^e
<i>r</i> -BN	A_1 : 770		E_1 : 1333	
	790 ^f		1367 ^f	

^aReference 5.

^dReference 16.

^bReference 13 and 14.

^eReference 17.

^cReference 15.

^fReference 8.

C. Phase transformation among *c*-BN, *h*-BN, *r*-BN, and *w*-BN

The analysis of our results in the previous sections lays a foundation for us to apply the stated calculation methodologies to the examination of several hypothetical phase transformation pathways among the four major polytypes of BN.

1. Simulation of simple direction compression

In this analysis, we start with a phase of BN in its stable equilibrium condition (Table I) and compress it with no change in lattice symmetry. The plots of energy vs volume for the four polytypes are shown in Fig. 5. The data show that the expansion of the atomic volumes of dense phases (*c*-BN and *w*-BN) and the compression of the light phases (*h*-BN and *r*-BN) both cost energy. These two types of phases have almost the same energy at 6.6 Å³. One can thus infer that a light phase such as *h*-BN or *r*-BN can be con-

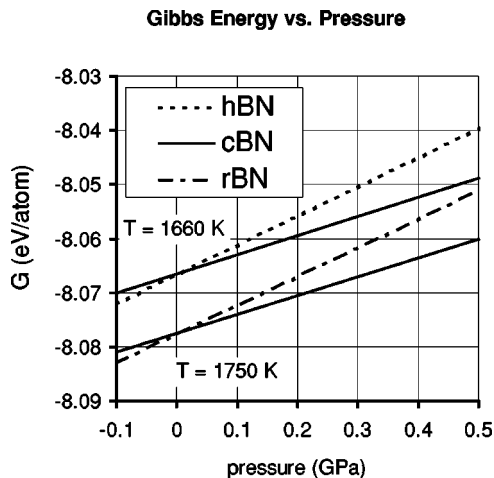


FIG. 3. Variation of Gibbs free energy vs pressure for *h*-BN/*c*-BN at temperature 1660 K and for *r*-BN/*c*-BN at temperature 1750 K.

Phase Boundaries of BN

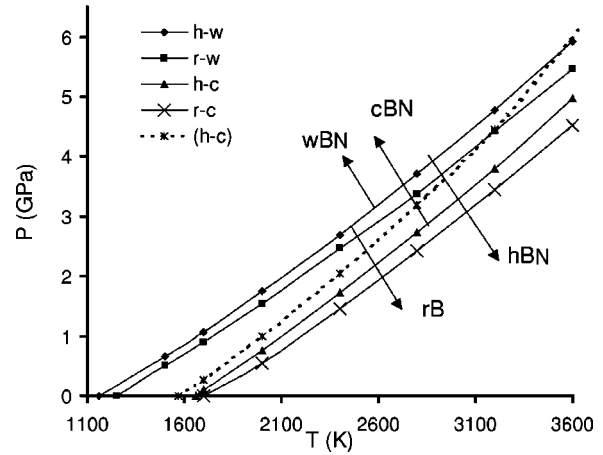


FIG. 4. *p*-*T* phase diagram of boron nitride. The diamond, square, triangle, and cross marked lines are the coexistence lines of *h*-BN/*w*-BN, *r*-BN/*w*-BN, *h*-BN/*c*-BN, and *r*-BN/*c*-BN, respectively, and the dashed line is the experimental curve of Solozhenko³.

tinuously compressed to an atomic volume of about 6.6 Å³, but for further shrinkage of atomic volume, the nature of energy minimization will drive its transformation to one of the dense phases.

In reality, the above simple direct compression is unlikely to preserve the lattice symmetry in the entire compression process, because in the presence of a given stress, the B and N atoms of a given phase will optimize its exact lattice structure to minimize its energy.

2. Simulation of conversion of *h*-BN to *w*-BN and *r*-BN to *c*-BN

As mentioned in the Introduction, the transformations between *h*-BN and *w*-BN and between *r*-BN and *c*-BN should not be too difficult. Simulations are conducted to examine these processes. The transformations of *h*-BN and *r*-BN by compression are simulated by reiterating the steps of (i)

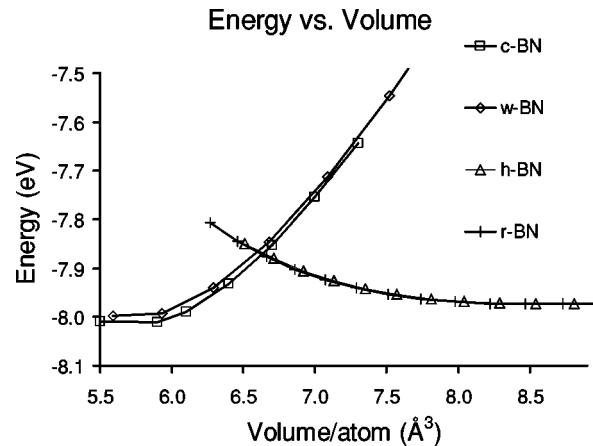


FIG. 5. Energy vs volume under compression with symmetry preserved for *c*-BN, *w*-BN, *h*-BN, and *r*-BN.

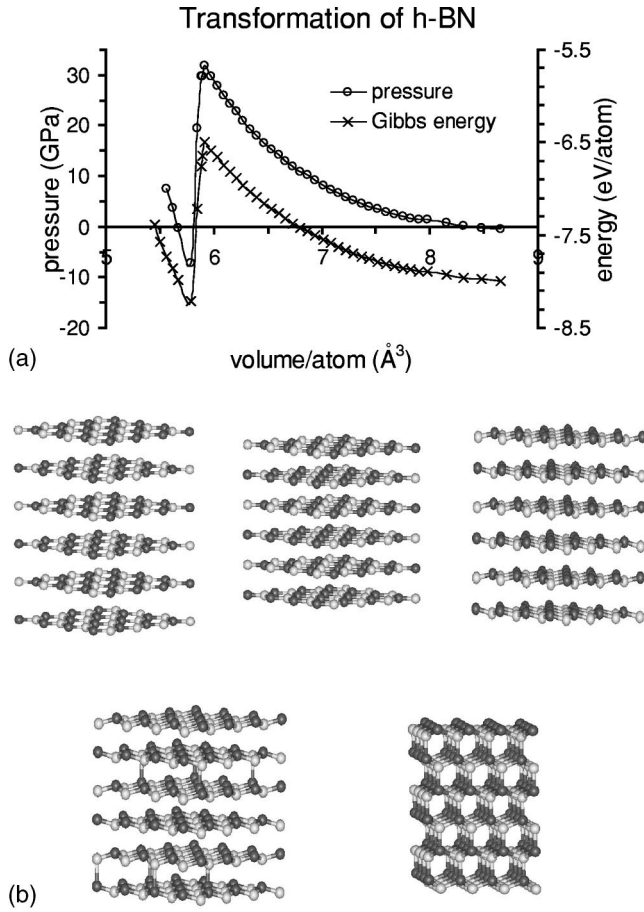


FIG. 6. (a) Correlations among pressure, volume, and energy during transformation between *h*-BN and *w*-BN by compression. (b) Structural changes during transformation between *h*-BN and *w*-BN by compression.

slightly reducing the cell volume without any change of the cell shape and (ii) optimizing the cell shape. The results for *h*-BN to *w*-BN are shown in Figs. 6(a) and 6(b). Clearly the geometry and symmetry of atoms on the basal planes do not change much initially, and the compression is reflected by the shrinkage of the basal plane separation. When the atomic volume approaches 5.8 \AA^3 , which requires a compression pressure over 30 GPa, the basal planes start buckling and a transformation to *w*-BN takes place. In a narrow range of atomic volume change, the internal stress reduces very rapidly and the conversion of *h*-BN to *w*-BN at its equilibrium configuration at $p=0$ is completed. For the compression of *h*-BN to 5.8 \AA^3 , an energy of about 1.4 eV/atom is required. The energy is quickly released when *w*-BN is formed. This is consistent with the data in Fig. 5, except that the data in Fig. 6 are more accurately calculated than those in Fig. 5.

A similar process for conversion of *r*-BN to *c*-BN is also seen in Figs. 7(a) and 7(b), which illustrate the transformation from *r*-BN to *c*-BN. The basal plane buckling takes place at the compressed volume of 6.2 \AA^3 .

The confirmation of the relative ease in transformation from *h*-BN to *w*-BN and *r*-BN to *c*-BN leads to the plausibility of a transformation mechanism for *h*-BN to *c*-BN by a

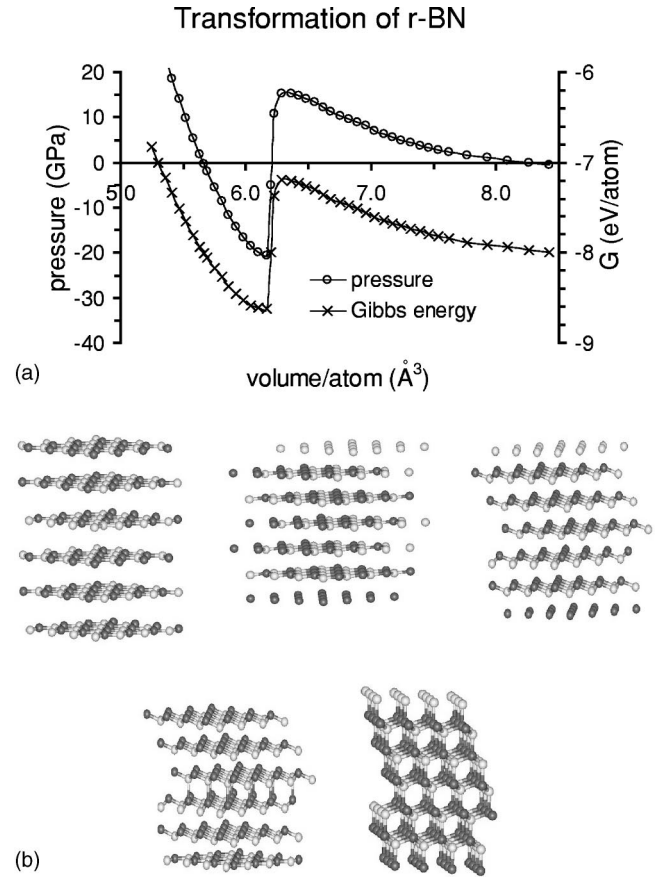


FIG. 7. (a) Correlations among pressure, volume, and energy during transformation between *r*-BN and *c*-BN by compression. (b) Structural changes during transformation between *r*-BN and *c*-BN by compression.

stepwise path of *h*-BN to *r*-BN and then to *c*-BN, or *h*-BN to *w*-BN and then to *c*-BN.

3. Transformation between *h*-BN and *r*-BN and between *c*-BN and *w*-BN

The transformations between *h*-BN and *r*-BN and between *c*-BN and *w*-BN are more difficult than those between *h*-BN and *w*-BN and between *r*-BN and *c*-BN. The difficulty is illustrated by the simulation data shown in Fig. 8 for *h*-BN to *r*-BN. In Fig. 8(a), the equilibrium structures of *h*-BN and *r*-BN are schematically compared and used as the starting and ending configurations in the simulation. The transformation is completed by the following operation: (i) fix the first (bottom) layer of atoms, (ii) rotate the second layer of atoms by $\pi/6$ round the *c* axis located at a B atom, (iii) translate the third layer of atoms by $a/2$, (iv) rotate the fourth layer of atoms by $\pi/6$ around the *c* axis, (v) translate the fifth layer of atoms by $-a/2$, and (vi) rotate the sixth layer of atoms by $-\pi/6$ around the *c* axis located at an N atom. The transformation path is simulated by partitioning the entire transformation process into several intermediate transformation steps such as those shown in Fig. 8. The energy diagram is shown in Fig. 9, together with other hypothetical transformation pathways. Since all these hypothetical transformation path-

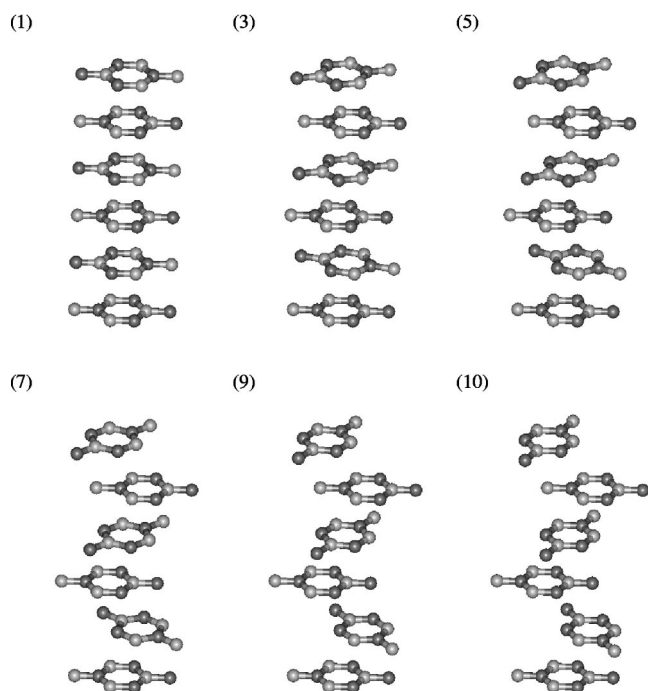


FIG. 8. Structural changes during transformation between *h*-BN and *r*-BN.

ways have not exhausted all transformation reaction configurations, the energy diagrams in Fig. 9 should only be interpreted as a collection of upper bounds of the energy barriers in the phase transformation of the BN system.

From the energy diagrams in Fig. 9, one can see that the energy barrier for direct phase transition from *h*-BN to *c*-BN is ~ 9.4 eV/atom, which is extremely high. In fact, even those between *h*-BN and *r*-BN and between *c*-BN and *w*-BN are formidably high. The results are consistent with the experimental data²⁰ of 6.5–10.8 eV/atom for direct conversion of *h*-BN to *c*-BN. A chemical reaction will certainly be kinetically barred when it has an energy barrier of more than 7 eV/atom. Therefore, the energy barrier data calculated in this study imply that the experimentally observed transformation from *c*-BN to *h*-BN does not follow the following three pathways summarized in Fig. 9: (i) direct transformation from

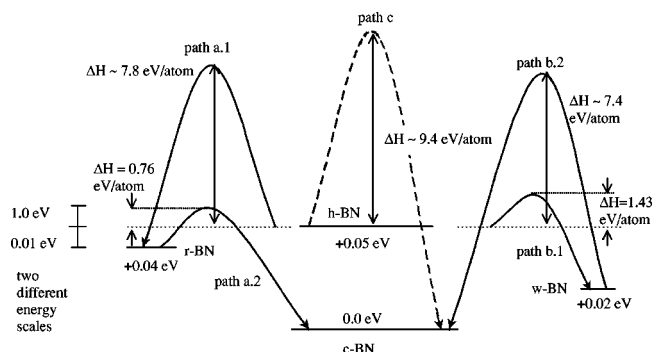


FIG. 9. Summary of the energy barriers of various paths in the phase transformations among *c*-BN, *r*-BN, *h*-BN, and *w*-BN (energy scale below the *h*-BN line is 100 times different from that above *h*-BN).

c-BN to *h*-BN, (ii) transformation from *c*-BN to *r*-BN and then to *h*-BN, and (iii) transformation from *c*-BN to *w*-BN and then to *h*-BN. On the same token, the data imply that there must be practical pathways other than those discussed in the above work.

In fact, the report of experimental data on the transformation from *c*-BN to *h*-BN did suggest that defects and impurities in *c*-BN might favorably drive the transformation.⁷ In the context of the present work, we propose that the incorporation of defects and impurities into the configurations of *c*-BN, *h*-BN and plausible transformation intermediates can reduce the energy barrier for the transformation sufficiently enough for it to proceed in conditions that can be achieved in common laboratories. For example, if the peripheral atoms of the planar clusters in Fig. 8 are terminated with hydrogen so that each cluster becomes a stand-alone planar molecule instead of a part of an infinitely large atom plane, the translation and rotational motions depicted in Fig. 8 will no longer be restricted by the corresponding high-energy barrier as shown in Fig. 9, because the plane-to-plane bonding is very weak. Indeed, we find an energy barrier of less than 0.5 eV/atom with the GAUSSIAN98 Revision A.7 codes²¹ and an MP2/6-31+*G*(*d*) basis set.

In practice, “defective” *h*-BN with sp^2 BN planes packed randomly is commonly observed in BN film growth and referred² to as turbostratic BN (*t*-BN). In addition, amorphous BN (*a*-BN), which does not possess any crystalline order, is commonly present, particularly at the beginning of BN film growth. Fine grains of *t*-BN in a nanometer scale and in a matrix of *a*-BN are expected to possess a low-energy barrier for the transformation between defective *t*-BN and defective *r*-BN and between defective *t*-BN and defective *h*-BN. Very recently Yang *et al.*²³ indeed showed by high-resolution transmission electron microscopy (HRTEM) the presence of *r*-BN and *h*-BN grains in a nanometer scale in the *t*-BN transition layer on which *c*-BN was grown in a BN film deposited on silicon.

D. Comparison with experimental data on *c*-BN film growth

A rather large experimental database on HRTEM of *c*-BN film growth^{2,23,24} has revealed a rather clear picture that a thin film of BN with *c*-BN as its main phase constituent can be grown on a convenient substrate such as silicon, with a phase composition transition from an interfacial layer of *a*-BN next to the substrate and then a transition layer containing mainly fine grains of *t*-BN with their sp^2 planes parallel to the growth direction. On the other hand, the strong correlation²⁵ between the presence of a highly compressive film stress and the growth of *c*-BN has already been generally accepted. The critical role of stress for *c*-BN formation has also been illustrated definitively by Yang *et al.*²³ in an HRTEM report, which gives a *t*-BN *d*-spacing contraction from 0.36 nm at the interface of *a*-BN/*t*-BN to 0.34 nm at the interface of *t*-BN/*c*-BN. In yet another experimental study in which the phase composition and stress of a *c*-BN film were measured as a function of the amount of film etching,²⁶ the presence of a compressive stress in the range 8 GPa–15 GPa

in the *c*-BN top layer, and a maximum compressive stress of 17 GPa in the *t*-BN transition layer were found. Hence, the conversion of defective *t*-BN to defective *r*-BN and then to defective *c*-BN, by processes similar to those depicted in Figs. 8 and 7, can indeed be a plausible *c*-BN growth pathway to reduce the energy barriers predicted in Fig. 9. Since *h*-BN, *r*-BN, and *c*-BN have very similar cohesive energies in their perfect bulk equilibrium configurations and since the atoms on a basal plane of *h*-BN or *r*-BN are very tightly bonded, defective *h*-BN (or *r*-BN) having defects in the basal planes will critically raise its energy and push the defective phase into a metastable state with energy higher than that of a defective *c*-BN phase. In addition, the presence of defects on the basal planes of *h*-BN (or *r*-BN) also effectively lowers the energy barrier for the transformation between *h*-BN and *r*-BN, which in turn effectively enhances the transformation probability between defective *h*-BN (or defective *r*-BN) and defective *c*-BN. Furthermore, Orellana and Chacham²⁷ showed recently, through first-principles calculations, that formation of native interstitials and vacancy-interstitial pairs are energetically easy in *h*-BN but difficult in *c*-BN. They suggested that during experimental growth of *c*-BN by ion bombardment assisted deposition, a preferential defect formation in *h*-BN favors the accumulation of *c*-BN. In the context of our present study, we see that ion bombardment is effective in generating defective *h*-BN which can relatively easily be transformed into defective *c*-BN, most possibly through compression. Once *c*-BN is formed, it is preferentially preserved, relative to *h*-BN, due to the defect dynamics depicted by Orellana and Chacham.

Finally, it is interesting that although defective *t*-BN, *h*-BN, and *r*-BN are all present in the *t*-BN transition layer and the energy difference between *c*-BN and *w*-BN is little, there has not been any experimental data showing the formation of *w*-BN as the main phase constituent in the BN layer grown on top of the *t*-BN transition layer with high film stress. It appears that all arguments used above for explaining the growth of *c*-BN on the *t*-BN transition layer can also

be used to support the prediction of the growth of *w*-BN. However, we note that as shown in Sec. III C 1, for the transformation from *h*-BN to *w*-BN, *h*-BN is needed to be compressed to an atomic volume of 5.8 \AA^3 at a pressure of about 32 GPa. In comparison, the transformation from *r*-BN to *c*-BN occurs at an atomic volume of 6.2 \AA^3 and at a pressure of 15 GPa. It is thus equivalent to say that the formation of *c*-BN effectively intercepts that of *w*-BN during ion-assisted BN film growth.

IV. CONCLUSION

In summary, the combination of the VASP codes and Parlinski's codes forms an effective computational analysis framework for the calculations of the *p*-*T* phase diagrams of polytypes of boron nitride. The results not only lead to clarification of the relative stabilities of these phases under different conditions, but also give us insights into the phase transformation among these phases. We learn from the results that a transformation between a dense phase and a light phase in their perfect bulk lattices will be difficult. Practical transformations have to proceed in the presence of defects, particularly defects in the basal planes of the light phases. Plausible defect aggregates include grain boundaries and dislocations. In addition, we also exemplify by compression simulations how the presence of internal stress helps the transformation from a compressed light phase to an expanded dense phase.

ACKNOWLEDGMENTS

The authors would like to thank Professor H. Q. Lin for his technical and scientific inputs in this work. The work was supported by the Chinese University of Hong Kong and the Research Grant Council of Hong Kong (RGC 4440/99E). We are grateful to the generous allocation of computer time from the High-Performance Computing System at the Information Technology Service Center of the Chinese University of Hong Kong.

*Corresponding author. Fax: 852-2994-3005. Electronic address: leol@cuhk.edu.hk

¹For a general review, see, e.g., E. Rapoport, *Ann. Chim. (Paris)* **10**, 607 (1985).

²For a review of *c*-BN films, see, e.g., P.B. Mirkarimi, K.F. McCarty, and D.L. Medlin, *Mater. Sci. Eng., R.* **21**, 47 (1997).

³V.L. Solozhenko, *J. Hard Mater.* **6**, 51 (1995).

⁴S. Bohr, R. Haubner, and B. Lux, *Diamond Relat. Mater.* **4**, 714 (1995).

⁵G. Kern, G. Kresse, and J. Hafner, *Phys. Rev. B* **59**, 8551 (1999).

⁶N. Ohba, K. Miwa, N. Nagasako, and A. Fukumoto, *Phys. Rev. B* **63**, 115207 (2001).

⁷H. Sachdev, R. Haubner, H. Nöth, and B. Lux, *Diamond Relat. Mater.* **6**, 286 (1997).

⁸J. Liu, Y.K. Vohra, J.T. Tarvin, and S.S. Vagarali, *Phys. Rev. B* **51**, 8591 (1995).

⁹D. Vanderbilt, *Phys. Rev. B* **41**, 7892 (1990).

¹⁰K. Parlinski, *J. Alloys Compd.* **328**, 97 (2001).

¹¹G. Kresse and J. Hafner, *Phys. Rev. B* **47**, 558 (1993); G. Kresse

and J. Furthmüller, *Comput. Mater. Sci.* **6**, 15 (1996).

¹²D. C. Wallace, *Thermodynamics of Crystals* (Wiley, New York, 1972).

¹³J.A. Sanjurjo, E. Lopez-Cruz, P. Vogl, and M. Cardona, *Phys. Rev. B* **28**, 4579 (1983).

¹⁴T. Weninghaus, J. Hahn, F. Richter, and D.R.T. Zahn, *Appl. Phys. Lett.* **70**, 958 (1997).

¹⁵R. Geick and C.H. Perry, *Phys. Rev.* **146**, 543 (1966).

¹⁶G. L. Doll, in *Properties of Group III Nitrides*, edited by J. M. Edgar (INSPEC, London, 1994), p. 245.

¹⁷K. Karch and F. Bechstedt, *Phys. Rev. B* **56**, 7404 (1997).

¹⁸V.L. Solozhenko and V. Ya Leonidov, *Russ. J. Phys. Chem.* **62**, 1646 (1988).

¹⁹F.A. Kuznetsov, A.N. Golubenko, and M.L. Kosinova, *Appl. Surf. Sci.* **113/114**, 638 (1997).

²⁰F.R. Corrigan and F.P. Bundy, *J. Chem. Phys.* **63**, 3812 (1975).

²¹M. J. Frisch *et al.*, computer code GAUSSIAN98, Revision A.7 (Gaussian Inc., Pittsburgh, PA, 1998).

²²A.V. Kurdyumov, V.L. Solozhenko, and W.B. Zelyavski, *J. Appl. Crystallogr.* **28**, 540 (1995).

- ²³H.S. Yang, C. Iwamoto, and T. Yoshida, J. Appl. Phys. **91**, 6695 (2002).
- ²⁴Q. Li, I. Bello, L.D. Marks, Y. Lifshitz, and S.T. Lee, Appl. Phys. Lett. **80**, 46 (2002).
- ²⁵D.R. McKenzie, W.D. McFall, W.G. Sainty, C.A. Davies, and R.E. Collins, Diamond Relat. Mater. **2**, 970 (1993).
- ²⁶S. Ilias, V. Stambouli, J. Pascallon, D. Bouchier, and G. Nouet, Diamond Relat. Mater. **7**, 391 (1998).
- ²⁷W. Orellana and H. Chacham, Phys. Rev. B **63**, 125205 (2001).